

Controlled domain-wall injection in perpendicularly magnetized strips

R. Lavrijsen,^{a)} J. H. Franken, J. T. Kohlhepp, H. J. M. Swagten, and B. Koopmans
Department of Applied Physics, Center for NanoMaterials and COBRA Research Institute, Eindhoven University of Technology, P.O. Box 513, 5600MB Eindhoven, The Netherlands

(Received 29 January 2010; accepted 3 May 2010; published online 1 June 2010)

For applications of domain wall (DW) motion in magnetic devices, it is vital to control the creation and position of the DW. We use Ga⁺ irradiation of Pt/Co/Pt strips to locally change the perpendicular magnetic anisotropy. This allows us to controllably inject DWs into a device at a tunable field. The observed initial linear decrease and subsequent increase in the DW injection field upon increasing irradiation dose are explained by micromagnetic simulations and an analytical one-dimensional model. © 2010 American Institute of Physics. [doi:10.1063/1.3432703]

Traditionally, the most studied system for domain wall (DW) motion is based on in-plane (IP) magnetized permalloy wires, which, due to a negligible magnetic anisotropy, exhibit wide and complex DWs.^{1–3} More reports have recently appeared on perpendicularly magnetized systems where the magnetization is oriented out-of-plane (OOP) due to a high perpendicular magnetic anisotropy (PMA).^{4–6} These seminal studies are mainly inspired by the prospect of low critical currents for current induced DW motion when dealing with narrow and simple Bloch type DWs.^{7,8}

For applications and research of DW motion in nanostructures, it is vital to precisely control the position where a DW is initially created/injected. For IP DW devices, this problem is easily overcome by demagnetization effects. Hence, a change of the local geometry can be used to locally lower the switching field, creating a reliable and reproducible way to create/inject DWs. This is, however, not viable for OOP systems since the PMA dominates over demagnetization effects. Surprisingly, this geometric approach is still widely used for PMA systems.^{4,9} By attaching a large nucleation pad to the device, the statistical chance to find an imperfection where a DW will nucleate at low field is increased. This naturally depends on the quality of the fabrication process and obviously does not lead to reliable and reproducible devices. Alternatively, it has been shown that low-dose irradiation by Ga⁺ ions leads to a reduction of the OOP anisotropy.^{10,11} Therefore, if only part of a structure is irradiated, this nucleation area switches first as demonstrated before.^{12,13} However, in these studies the magnetic field needed to depin a DW from such an irradiated area has not been further investigated.

In this paper, we study the effect of local irradiation of a Pt/Co/Pt strip for DW injection. We will present a systematic analysis of the injection field H_{in} needed to inject a DW into a device as function of Ga⁺ dose. Interestingly, we observe that H_{in} sharply decreases under low Ga⁺ dose, but then increases again with increasing dose due to DW pinning. This counterintuitive behavior is shown to match well with micromagnetic simulations and is additionally supported by a simple analytical one-dimensional (1D) DW model, allowing to tune and predict H_{in} . We anticipate that the proposed way to introduce DW injection points and engineered DW pin-

ning sites will accelerate the research and device implementation of PMA materials.

The devices under investigation are shown in the sketch of Fig. 1(a). The strips consist of Pt(4 nm)/Co(0.6 nm)/Pt(2 nm) patterned by electron beam lithography, lift-off, and grown by dc-sputtering on a Si/SiO₂ substrate. Prior to electrical contacting, the Hall cross is partly irradiated [see sketch Fig. 1(a)] with a varying dose of Ga⁺ ions (0.1–5.0 $\mu\text{C}/\text{cm}^2$ with beam settings: 30 keV, 2 pA) with a focused ion beam (FIB).

To verify that the magnetization reversal is initiated in the Ga⁺ irradiated area we use polar Kerr microscopy.¹⁴ In Fig. 1(a) a sequence of Kerr images is shown for increasing applied field. One can clearly see that with increasing field (4.4–6.8 mT) the irradiated area starts to reverse its magnetization by progressive nucleation and expansion of domains, indicating that the Ga⁺ irradiation generates local nucleation sites where domains are easily nucleated at low field due to the lowered anisotropy. At 6.9 (7.7) mT the left (right) DW depins followed by the reversal of the left (right) part of the structure by DW motion. This process is reproducible but the depinning field varies slightly due to the stochasticity induced by thermal activation. We define H_{in} as the average of the depinning field of the right and left DW.

We can sensitively measure the OOP magnetization in the Hall cross when we electrically contact the sample (lock-in detection, $I_{ac}=10 \mu\text{A}$) by the extraordinary Hall effect (EHE). This is shown in Fig. 1(b) where partial hysteresis loops are shown of Hall crosses irradiated with different doses. Three regimes can be distinguished: (i) at the lowest dose (0.1 $\mu\text{C}/\text{cm}^2$) the hysteresis loop shape is similar to a non-irradiated sample (not shown). The square hysteresis loop indicates that the reversal mechanism is dominated by thermally activated domain nucleation at a certain imperfection and consecutive fast DW motion through the device. (ii) When we increase the dose to 0.6 $\mu\text{C}/\text{cm}^2$, a sharp reduction is seen in the start of the reversal, and H_{in} is greatly reduced. Furthermore, small steps are seen directly above $\mu_0 H=0$. This corresponds to the reversal taking place by a few small domains nucleating in the irradiated area of which the reversal is completed at around ≈ 8.6 mT. The large steps at ≈ 9.3 mT indicates the depinning of the right and left DW from the boundaries into the device, similar to what we have seen in Fig. 1(a). (iii) At a dose of 1.5 $\mu\text{C}/\text{cm}^2$ we do not observe the small steps corresponding to the reversal

^{a)}Electronic mail: r.lavrijsen@tue.nl.

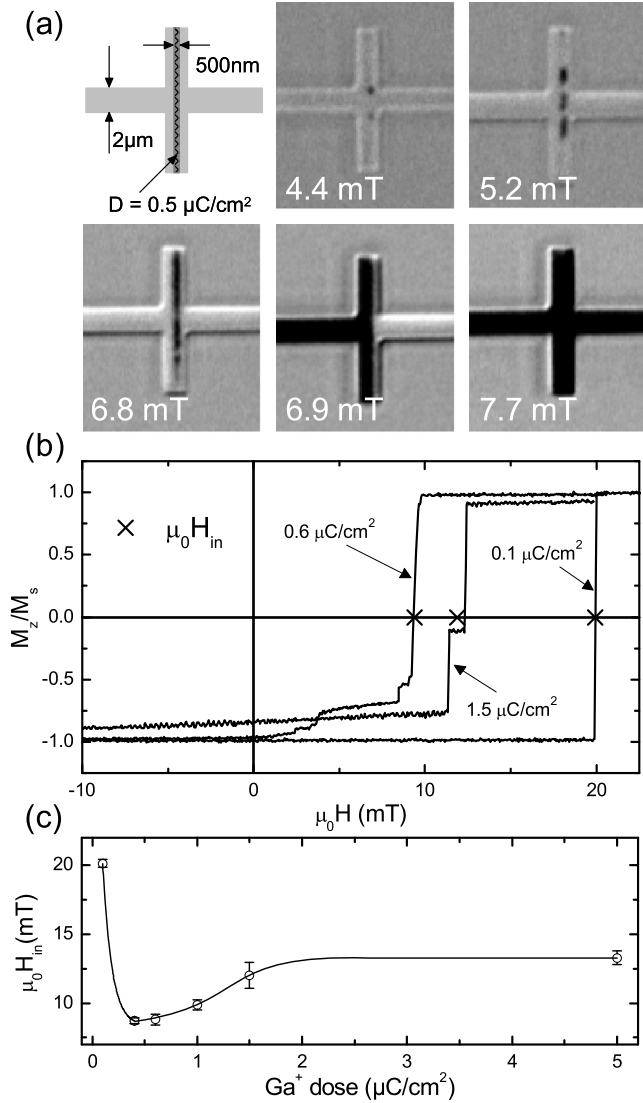


FIG. 1. (a) A sketch of the samples used and Kerr microscopy images of a sample irradiated with a dose of $0.5 \mu\text{C}/\text{cm}^2$; the gray (black) contrast corresponds to the magnetization pointing up (down). (b) Normalized EHE hysteresis loops for Hall crosses irradiated with different doses; the \times 's indicate H_{in} . (c) H_{in} as a function of Ga^+ dose determined from 20 measurements; the error bar shows the standard deviation, the line is a guide to the eye.

of the irradiated area. Instead of the steps we observe a reduction of the remanence and a gradual slope around zero field, indicating that the magnetization is IP and the field is pulling the moments OOP. But more surprisingly, H_{in} has increased to 11.9 mT where the plateau around H_{in} indicates the different depinning fields of the left and right DWs from the boundary. In Fig. 1(c) H_{in} is plotted as function of dose showing the initial sharp decrease followed by a gradual recovery at higher dose.

To explain this peculiar behavior of H_{in} , micromagnetic simulations¹⁵ are performed. A small strip [$400 \times 60 \times 1 \text{ nm}^3$, shown in the inset of Fig. 2(b)] discretized in $4 \times 4 \times 1 \text{ nm}^3$ cells is split into two parts. The left part has a fixed effective OOP anisotropy $K_{\text{eff},0} = K_0 - 1/2 \mu_0 N_z M_s^2 = 305 \text{ kJ}/\text{m}^3$, taking $K_0 = 1.5 \text{ MJ}/\text{m}^3$, $M_s = 1400 \text{ kA}/\text{m}$, a demagnetizing factor of $N_z = 0.96$, and an exchange stiffness $A = 16 \text{ pJ}/\text{m}$.¹⁶ The right part of the strip, which mimics the irradiated area of our experiments, has a reduced anisotropy $K_{\text{eff}} < K_{\text{eff},0}$. For now we assume a sharp boundary described by the boundary width $\delta = 0$.

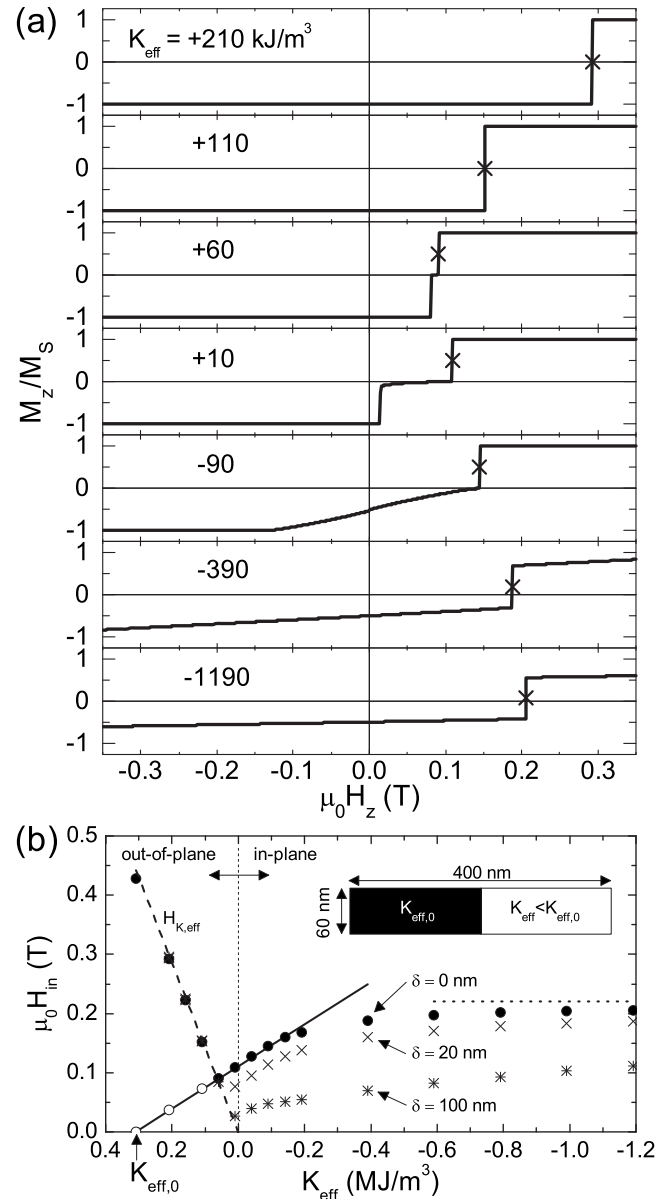


FIG. 2. (a) Simulated hysteresis loops of a $400 \times 60 \times 1 \text{ nm}^3$ strip, where half of the area has a reduced anisotropy $K_{\text{eff}} < K_{\text{eff},0}$ and the other half has a fixed anisotropy $K_{\text{eff},0} = 305 \text{ kJ}/\text{m}^3$ as shown in the inset of (b). H_{in} is indicated by the \times 's. (b) H_{in} obtained from (a). The dashed line shows the effective anisotropy field $H_{K_{\text{eff}}}$. The solid (dotted) line is obtained from the 1D model assuming a full (rescaled) Bloch profile. The open circles are simulations, starting with an artificially prepared DW at the boundary. The crossed symbols correspond to H_{in} with different boundary widths δ .

In Fig. 2(a) simulated quasistatic OOP hysteresis loops taken over the whole structure are shown for different K_{eff} . A positive (negative) K_{eff} indicates an OOP (IP) easy axis. A trend can be observed with decreasing K_{eff} , viz. from a square hysteresis loop for $K_{\text{eff}} > +110 \text{ kJ}/\text{m}^3$, to a loop with a double step for $+60 > K_{\text{eff}} > +10 \text{ kJ}/\text{m}^3$ and finally a slanted loop with a single step when $K_{\text{eff}} < 0$.

Starting with a high K_{eff} (top) we find, as expected, a square hysteresis loop with a sharp switch at the anisotropy field $H_{K_{\text{eff}}} = 2K_{\text{eff}}/(\mu_0 M_s)$. The \times 's indicate the field at which the $K_{\text{eff},0}$ area reverses its magnetization and thus corresponds to H_{in} . The reversal always proceeds by a domain that is nucleated in the $K_{\text{eff}} < K_{\text{eff},0}$ region. When the DW arrives at the boundary the field is high enough to push the DW into the $K_{\text{eff},0}$ region and this region will also reverse by fast DW

motion. For $+60 < K_{\text{eff}} < +10 \text{ kJ/m}^3$ we observe an extra step in the hysteresis loop which corresponds to the DW getting pinned at the boundary, i.e., a higher field is needed to push the DW into the $K_{\text{eff},0}$ region indicated by the extra step. When $K_{\text{eff}} < 0$ we lose the well-defined perpendicular magnetization in the area with reduced K_{eff} . This is seen by the slope around zero field and the loss of 100% remanence. In Fig. 2(b), H_{in} obtained from the simulations ($\delta=0$) is plotted as a function of K_{eff} . For $K_{\text{eff}} > 60 \text{ kJ/m}^3$, H_{in} is linear with anisotropy and exactly corresponds to the anisotropy field $\mu_0 H_{K_{\text{eff}}}$ (dashed line). When $K_{\text{eff}} \leq +60 \text{ kJ/m}^3$, DW pinning at the boundary dominates the injection field and H_{in} increases again.

In the experiment the sharpness of the boundary is limited by the Ga^+ beam profile specified to be 7 nm at FWHM. The width of the DW pinning potential at the boundary is governed by the DW width $\Delta = \sqrt{A/K_{\text{eff},0}} = 7.2 \text{ nm}$, i.e., they are of the same order. To investigate the effect of the beam profile in the simulations we implemented a linear change (stepwise in the cells) of the anisotropy at the boundary, with a boundary width of $\delta = 20$ and 100 nm. The results are shown in Fig. 2(b). Again, a similar behavior is found, although with an overall reduced H_{in} and a more gradual increase in H_{in} for DW pinning at the boundary.

Comparing to the experimental data of Fig. 1(c), a very good qualitative correspondence of H_{in} is seen where a higher Ga^+ dose corresponds to a lower K_{eff} . The magnitude of H_{in} is, however, much lower in the experiment due to thermal activation processes playing a crucial role as is well known for these materials.^{16,17}

We now concentrate on the anisotropy regime where H_{in} starts to increase due to DW pinning at the boundary i.e., $K_{\text{eff}} < 60 \text{ kJ/m}^3$. Let us assume the 1D Bloch DW obeys the well-known profile,¹⁸ i.e., the OOP angle θ along the wire axis x is given by: $\theta(x) = \pm 2 \arctan[\exp(x/\Delta)]$. The DW energy per unit area is then given by $E_{\text{DW}} = 4\sqrt{AK_{\text{eff}}}$. Hence, the DW has to overcome a certain energy barrier to propagate into the $K_{\text{eff},0}$ region. The energy landscape felt by the DW can be tilted by the Zeeman energy of an applied field pushing the DW into the $K_{\text{eff},0}$ region as soon as the tilt slope cancels the maximum slope of the DW energy landscape. Assuming that the magnetization is OOP in both regions and the DW retains a Bloch profile, we find analytically that $H_{\text{in}} = (K_{\text{eff},0} - K_{\text{eff}}) / (2\mu_0 M_S)$, as is shown in Fig. 2(b) by the solid line. It corresponds exactly to the simulated data for $+60 < K_{\text{eff}} < -140 \text{ kJ/m}^3$, confirming that the assumed Bloch profile is reasonable. When we implement $\delta > 0$ into the 1D model to mimic the finite Ga^+ beam width, we analytically find (assuming a linear change in the anisotropy) that the pinning at the boundary (solid line) is reduced by a factor $(2\Delta_{\text{eff}}/\delta)\tanh(\delta/2\Delta_{\text{eff}})$. This factor corresponds with the observed reduction in H_{in} found from micromagnetic simulations [Fig. 2(b), crossed symbols]. In that case, an effective DW width Δ_{eff} is used, obtained from a fit to the pinned DW profile.

When $K_{\text{eff}} < -140 \text{ kJ/m}^3$ the pinning model starts to deviate from the simulated data due to an increasing IP character of the magnetization in the low K_{eff} region, indicating that the assumed Bloch profile is no longer valid. For $K_{\text{eff}} \ll 0$ we can make a crude assumption by rescaling the Bloch

profile from $\theta \in [0, \pi]$ to $\theta \in [0, \frac{\pi}{2}]$ giving $\theta(x) = \pm \arctan[\exp(x/\Delta)]$. Using a similar analysis as above with an OOP (IP) easy axis in the $K_{\text{eff},0}$ (K_{eff}) region, we find $H_{\text{pin}} = K_{\text{eff},0} / \mu_0 M_S$. This relation is shown as the dotted line in Fig. 2(b) and matches the asymptotic behavior of the micromagnetic simulations. The small offset between the simulation and the model is due to the field already present at H_{in} tilting the moments OOP in the K_{eff} region which is not taken into account in the profile. Finally, from the above analysis a minimal injection field can be found from the intersection of $H_{K_{\text{eff}}}$ and H_{in} found around $K_{\text{eff}} = 60 \text{ kJ/m}^3$. This is given by $H_{\text{in,min}} = 2/5 \times K_{\text{eff},0} / \mu_0 M_S$, giving at least a qualitative handle to tune $H_{\text{in,min}}$.

In this paper, it is demonstrated that Ga^+ irradiation can be used to controllably depin a DW in a perpendicularly magnetized Pt/Co/Pt strip which we substantiated by micromagnetic simulations and a simple analytical 1D DW model. The ease and tunability of the technique makes us believe that it will greatly stimulate the field of DW physics and devices.

We thank NanoNed, a Dutch nanotechnology program of the Ministry of Economic Affairs. Collaboration with Christine Hamann, Rudolf Schafer, and Jeffrey McCord is highly appreciated. This work is part of the research program of the Foundation for Fundamental Research on Matter (FOM), which is financially supported by the Netherlands Organization for Scientific Research (NWO).

¹M. Kläui, *J. Phys. D* **20**, 313001 (2008).

²S. S. P. Parkin, M. Hayashi, and L. Thomas, *Science* **320**, 190 (2008).

³M. Hayashi, L. Thomas, R. Moriya, C. Rettner, and S. S. P. Parkin, *Science* **320**, 209 (2008).

⁴C. Burrowes, A. Mihai, D. Ravelosona, J.-V. Kim, C. Chappert, L. Vila, A. Marty, Y. Samson, F. Garcia-Sanchez, and L. Buda-Prejbeanu, *Nat. Phys.* **6**, 17 (2010).

⁵T. A. Moore, I. M. Miron, G. Gaudin, G. Serret, S. Auffret, B. Rodmacq, A. Schuhl, S. Pizzini, J. Vogel, and M. Bonfim, *Appl. Phys. Lett.* **93**, 262504 (2008).

⁶O. Boulle, J. Kimling, P. Warnicke, M. Kläui, U. Rudinger, G. Malinowski, H. Swagten, B. Koopmans, C. Ulysse, and G. Faini, *Phys. Rev. Lett.* **101**, 216601 (2008).

⁷S. Zhang and Z. Li, *Phys. Rev. Lett.* **93**, 127204 (2004).

⁸G. Tatara and H. Kohno, *Phys. Rev. Lett.* **92**, 086601 (2004).

⁹D. Ravelosona, D. Lacour, J. Katine, B. Terris, and C. Chappert, *Phys. Rev. Lett.* **95**, 117203 (2005).

¹⁰A. Aziz, S. J. Bending, H. Roberts, S. Crampin, P. J. Heard, and C. H. Marrows, *J. Appl. Phys.* **98**, 124102 (2005).

¹¹R. Hyndman, P. Warin, J. Gierak, J. Ferré, J. N. Chapman, J. P. Jamet, V. Mathet, and C. Chappert, *J. Appl. Phys.* **90**, 3843 (2001).

¹²L. San Emeterio Alvarez, G. Bernell, C. H. Marrows, K.-Y. Wang, A. M. Blackburn, and D. A. Williams, *J. Appl. Phys.* **101**, 09F508 (2007).

¹³A. Aziz, S. J. Bending, H. G. Roberts, S. Crampin, P. J. Heard, and C. H. Marrows, *Phys. Rev. Lett.* **97**, 206602 (2006).

¹⁴The Kerr images have been obtained at the Leibniz Institute for Solid State and Materials Research (IFW Dresden).

¹⁵M. R. Scheinfein, LLG micromagnetics simulator™, <http://llgmicro.home.mindspring.com/>.

¹⁶P. J. Metaxas, J. P. Jamet, A. Mougou, M. Cormier, J. Ferré, V. Baltz, B. Rodmacq, B. Dieny, and R. L. Stamps, *Phys. Rev. Lett.* **99**, 217208 (2007).

¹⁷C. Burrowes, D. Ravelosona, C. Chappert, S. Mangin, E. E. Fullerton, J. A. Katine, and B. D. Terris, *Appl. Phys. Lett.* **93**, 172513 (2008).

¹⁸A. Hubert and R. Schäfer, *Magnetic Domains* (Springer, Santa Clara, 1998).